Journal of Coastal Conservation (2023) 26:5
https://doi.org/10.1007/s11852-023-00934-2

Influence of land cover indices and surface temperature on the metals bioaccumulation by three Macrophytes in Lake Burullus, Egypt

Muhammad A. El-Alfy[1] · Mamdouh S. Serag[2] · Afifi I. Basiony[1] · Mohamed Fathi[3] · Dina H. Darwish[1]

Received: 29 September 2022 / Revised: 29 December 2022 / Accepted: 17 January 2023 / Published online: 2 February 2023

Abstract

Nowadays, the importance of using macrophytes in accumulation of heavy metals has gained great concerns. So, this study aimed at extracting the land use/cover types of three indices and surface temperatures in the habitats inside 100 m buffers from recent satellite images around three highly economic macrophytes namely; *Phragmites australis, Typha domingensis* and *Potamogeton pectinatus* species. In addition to land surface temperature (LST), three important indices expressing the land cover of habitats namely; normalized different vegetation index (NDVI), normalized different water index (NDWI), and normalized different moisture index (NDMI) were extracted to find out there influence on the efficiency of macrophytes in the accumulation of these metal ions; Fe, Cu, Zn, Cd and Pb. The Polynomial regression models were calculated to predict the accumulation factors of plants within the remotely sensed indices and LST. Results showed different accumulation values for individual or more metals in the below-ground and above-ground parts of macrophytes within different habitats. This study considers as an innovative approach using remote sensing technique and satellite images for the selecting of species that can accumulate more metals within different habitats. The obtained results will be useful for the optimal management of these macrophytes in Lake Burullus, a Ramsar site.

Keywords Land surface temperature (LST) · Macrophytes · Land cover indices · Ramsar site · Reeds and metal ions

Introduction

Heavy metals in the environment have become a global issue due to the increase of human impact (Dar et al. 2020; Nabi 2021). They are severe contaminants in environments due to their persistence, toxicity, and bioaccumulation (Nabi and Dar 2022). Wetlands and coastal waters are ecosystems that are particularly vulnerable to heavy metal inputs (Mitsch and Gosselink 2007; Halpern et al. 2008). Natural processes typically do not remove heavy metals from these ecosystems (Bargagli 1998). As soon as heavy metals get accumulate in bottom sediments, they begin to move up the food chain, often biomagnifying at higher trophic levels and ultimately causing potential disorders in humans and animals (Barwick and Maher 2003; Roberts et al. 2008). Recently, there has been awareness towards using biological indicators such as plants for monitoring and quantifying different pollution types (air, water, and soil) (Al-Yemni et al. 2011). Plants have the ability to absorb all metals, especially those essential for their growth and development (Kabata-Pendias 2011). Macrophytes, in particular, play a fundamental role in wetland geochemistry because they are the principal living accumulators of heavy metals through active and passive absorption (Vodyanitskii and Shoba 2015; Dar et al. 2022a). They show significant variety in their accumulative capacities to heavy metals and transfer them to above-ground organs (Baldantoni et al. 2009).

✉ Muhammad A. El-Alfy
muhammad.elalfy@yahoo.com; ma.elalfy@niof.sci.eg

Mamdouh S. Serag
mamdouhserag054@gmail.com

Afifi I. Basiony
abasiony38@yahoo.com

Mohamed Fathi
mfnagar@yahoo.com

Dina H. Darwish
marawan.dina@yahoo.com

[1] National Institute of Oceanography and Fisheries, NIOF, Cairo, Egypt

[2] Botany and Microbiology Department, Faculty of Science, Damietta University, New Damietta City, Egypt

[3] Limnology Department, Central Laboratory for Aquaculture Research, Agricultural Research Centre, Abbassa, Egypt

Aquatic macrophytes are aquatic vascular plants that are broadly distributed in several wet environments, from freshwater to saltwater. The shallow areas of lakes, ponds, pools, marshes, streams, and rivers are where aquatic macrophytes are most frequently found (Dar et al. 2022b). They may be emergent, submerged or floating, rooted or unrooted in habit, with associated adaptations to the leaves, stems and/or roots matching the requirements of these aquatic environments (Bornete and Puijalon 2011; Peters and Lodge 2009; Rejmankova 2011). The spread of macrophytes affects the water circulation and subsequently may affect the quality of the water and fish in the lake. These plants are considered a huge source of raw material for industrial production of paper pulp, biofuel and natural therapeutics (Dar et al. 2021a, b). Besides, aquatic macrophytes have shown high efficiency to remove pollutants and recover nutrients from a wide variety of domestic, industrial and agricultural effluents, which validates their role in the bio-remediation of polluted water (Serag 1996; Haroon 2022).

Land surface temperature (LST) represents an important factor in global climatic change and is used in the applications of various fields such as meteorology, climatology and hydrology. Also, the change of land use/cover (LU/LC) has been long established to have an impact on the climate through variable features that modulate precipitation and LST. LULC, on the other hand, produces an impression that may affect the earth's energy balance, thereby altering the region's climate. One of the most common modifiers is LST (Solanky et al. 2018; El Garouani et al. 2021; Ovalle et al. 2021).

This study aimed to investigate the effect of land surface temperature and different land cover types in the surrounding plant habitats on the accumulation efficiency of metal ions in Lake Burullus, a Ramsar site.

Materials and methods

Study area

Lake Burullus extends along the Egyptian Deltaic Coast of Mediterranean sea from latitude 31° 15′ N to 31° 40′ N and from longitude 30° 20′ to 31 10′E (Fig. 1). It is located between Damietta and Rosetta branches of River Nile, and considers one of the largest natural lakes in Egypt after Lake Manzala, covering an area of 420 km^2. It has a rectangle shape covers a distance of 47 km along the NE-SW axis with a width ranging between 4 and 14 km (Okbah 2005; Shaltout and Khalil 2005). The northeastern edge of the Lake has a short canal called Boughaz El-Burullus that connects it to the Mediterranean Sea, through which sea water comes into the lake easily during the periods of low Nile water inflows. The lake is known for its many islands, and the majority of these islands run from south to north (Abd el-Sadek et al. 2022). Other islands are either parallel or perpendicular to the current shore. Lake Burullus is home to about seventy five islands with different habitat types (Balah 2012). Many floating vegetation types, such as reeds and submerged in the lake, altering the water circulation. These plants serve as a vital role in preventing the collapse of the lake's interior shores (Abd el-Sadek, et al., 2022). The area of Lake

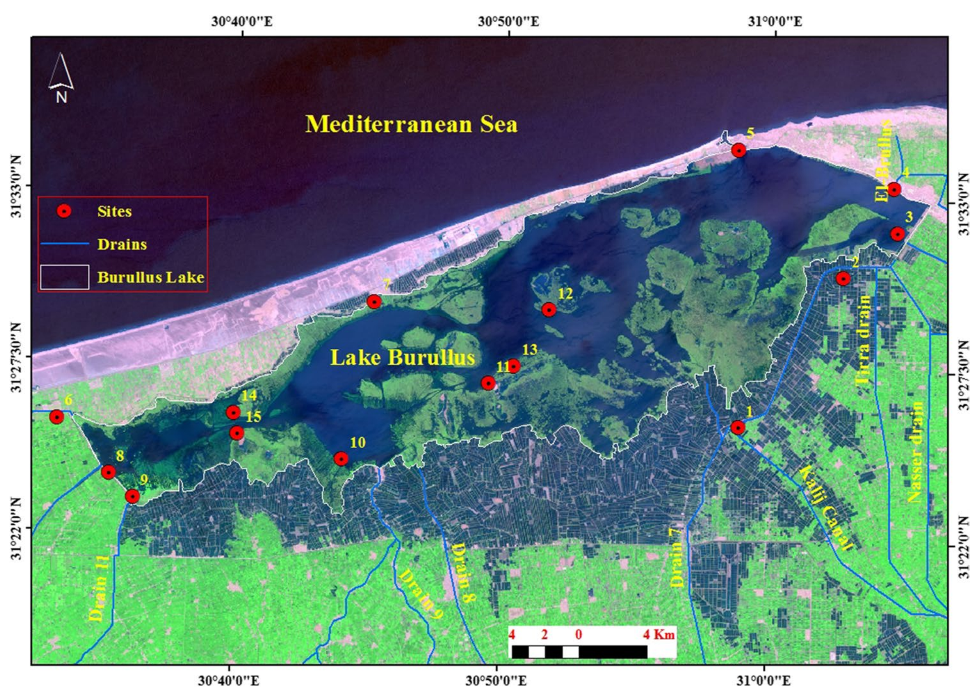

Fig. 1 Sampling sites within and around the Lake Burullus

Burullus has changed as a result of shrinking that led to the increase in islands size (Khedr 1999; Balah 2012).

The northern Mediterranean part of the Nile Delta belongs to the arid zone as shown by the world distribution map of arid regions. As a result, Lake Burullus is characterized by an arid climate with temperatures range between (20–30° C) and (10–20° C) in warm summers and mild winters, respectively (UNESCO 1977; UKMO, 2013).

Lake Burullus receives drainage water from seven drains along its southern edge and freshwater from the Brinbal Canal in its southwest corner (Okbah and Hussein 2006). The amount of drainage waters coming from agricultural lands to Lake Burullus equal to nearly 4 billion m^3/year (El Shinnawy, 2002), which accounts for 97% of the water inflow (Shaltout and Khalil 2005; Eid 2012). Lake Burullus is affected by agricultural drainage water assorted with different types of drained waters from fish ponds, and industrial and municipal wastewater discharges through the drains.

Ecological and botanical description of macrophytes

Aquatic plants including *Phragmites australis, Typha domingensis* and *Potamogeton pectinatus*; are macrophytes that are distributed all over the world. These species are rhizomatous perennial herbaceous plants that grow in condensed mono-specific stands in natural lakes with stagnant, shallow water and, sediments of muddy nature (Pignatti 1982). These plants have been employed to detect, monitor, and remediate water contamination (Wolverton and McDonald 1978; Peng et al. 2008; Bonanno and Giudice 2010; and Eid et al. 2012).

i *Phragmites australis*: It is believed to be one of the most widely distributed species in the world (Holm et al. 1977). In Egypt, *Phragmites australis* occurs in all phytogeographical areas (Täckholm 1974; Zahran and Willis 2009; Boulos 2005). It has found in the main habitats of the Lake Burullus area including: salt marshes, sand sheets, lands that have been cut off from the lake, terraces, slopes, and water edges as well as open water zones of drains, lake shores and the open water of the lake (Shaltout and Al-Sodany 2008). It is an emergent plant and one of the important macrophytes. It is a perennial reed that grows from elongated rhizomes or stolons. It is 1–6 m tall, and forms dense stands. Stems are erect, hollow, reed-like, simple, 150–600 cm long, 5–15 mm thick and hollow internodes. Leaves are linear, flat, drooping, and leaf blades are deciduous at the ligule; 20–60 cm long; 8–32 mm wide, with pointed tips. Flowers happen in August and September and form bushy panicles (Clayton et al. 2006; Klein 2011). *Phragmites australis* forms a dense network of roots and rhizomes that can go down up to two meters in depth to reach deep groundwater (MA DCR 2002). It grows in marshes and swamps, along streams, lakes, ponds, ditches, and wet wastelands, often weedy and very difficult to eradicate. It grows best in firm mineral clays and tolerates moderate salinity, where the water level varies from 15 cm below the soil surface to 15 cm above. Ranging from cool temperate steppe to wet through the tropical desert to moist forest life zones, the reed is reported to tolerate annual precipitation of 3.1 to 24.1 dm, the annual temperature of 6.6 to 26.6 ºC and pH of 4.8 to 8.2 (Duke 1978, 1979). Besides, the reed tolerates soil conductivity up to 12 mS cm-1 and pH 7.0 to 9.3 (Serag, 1996). *Phragmites australis* has been used as a bio-indicator for heavy metals, and to store heavy metals to some extent (Bonanno 2011; Salem et al. 2014; Morari et al. 2015).

ii *Typha domingensis* is an emergent plant native to warm temperate and tropical climates that grows in ditches and marshy areas all across Egypt. (Täckholm 1974; Boulos 2005).). It is an erect, perennial, freshwater macrophyte that can grow 3 or more meters in height. The linear cattail leaves are thick, ribbon-like structures with a spongy cross-section exhibiting air channels. The subterranean stem arises from thick creeping rhizomes (Smith 1962, 1967). *Typha domingensis* is one of the main components of vegetation that stands along the shores of Lake Burullus close to the Deltaic Mediterranean coast (Shaltout and Al-Sodany 2008). *Typha domingensis* is used in constructed wetlands for the enhancement of water quality (Abdel-Ghani et al. 2009) due to its high growth rate and great capacity for heavy metal accumulation (Newman et al. 1996; Lorenzen et al. 2001).

iii *Potamogeton pectinatus* is a submerged perennial aquatic macrophyte (Boulos 2005) with a parvopotamid growth form (Hogeweg and Brenkert 1969). It is characterized by slender round shoots up to 3 m long with narrow linear leaves (Kłosowski and Kłosowski 2007). It also occurs in almost all climatic areas and has a widespread distribution (Pilon et al. 2002), and occurs in a variety of habitats including water of different trophic levels, standing and running water, alkaline, fresh and brackish waters. (van Wijk 1988). It can survive in environments with high salinity and pollution (Casagranda and Boudouresque 2007).

Site description and sampling protocol

Samples were collected from fifteen stations in two locations (Table 1; Fig. 1);

i. Burullus Lake shores comprise ten sampling sites; Drain 7 (in front of drain No. 7), Maktoaa, Brinbal, Khashaa, West/Tirrah, West/El-Burullus, Boughaz, East/El Burullus, El Hoks, and EL Shakhlouba.

ii. Burullus Lake islets comprise five sampling sites; Ebsak, Maksaba, Elkome Elakhdar, Abu-Amer, and Deshemy (Fig. 2).

Sampling protocol

Fifteen sampling sites were selected along Lake Burullus. Samples considered were water, sediments and plant. The samples of water, sediments, and macrophytes were collected from the same sites. The sampling program was conducted during the summer season of the years 2020 and 2021, respectively.

Water sampling

Water samples were collected from various locations along the shoreline and islets of Burullus Lake (Table 1; Fig. 1). The collected water samples were kept in an ice box, then, it was transferred to the laboratory for heavy metals determination.

Sediment sampling

Surface sediment samples were collected using a Van-Veen grab coated with polyethylene (Amini Ranjbar 1998), and analyzed for Fe, Cu, Zn, Cd, and Pb. The samples were kept in plastic bags and transported to the laboratory, air-dried at room temperature and stored in plastic bags until analysis.

Table 1 Latitudes and longitudes of sampling sites

Location	Site	NO	Latitudes	Longitudes
Lake Shore	Drain 7	1	31° 25′ 42.40″	30° 58′ 52.80″
	West Tirra	2	31° 30′ 33.00″	31° 02′ 44.80″
	El-Kashaa	3	31° 32′ 01.70″	31° 04′ 45.00″
	Burullus/East	4	31° 33′ 27.40″	31° 04′ 34.60″
	El-Boughaz	5	31° 34′ 44.20″	30° 58′ 04.20″
	Burullus/West	6	31° 25′ 37.60″	30° 33′ 22.10″
	El-Maksaba	7	31° 29′ 31.90″	30° 45′ 11.20″
	Brinbal	8	31° 24′ 03.20″	31° 35′ 06.00″
	El-Hoks	9	31° 23′ 06.80″	30° 36′ 17.00″
	El-Shaklouba	10	31° 24′ 27.40″	30° 44′ 03.40″
Islets	El-Kome El-Akdar	11	31° 26′ 58.70″	30° 49′ 30.60″
	Besak	12	31° 29′ 22.60″	30° 51′ 44.10″
	El-Maktoaa	13	31° 27′ 32.50″	30° 50′ 25.90″
	Abu-Amer	14	31° 25′ 53.30″	30° 39′ 58.20″
	Deshemy	15	31° 25′ 13.12″	30° 40′ 09.10″

Plant sampling

At each sampling point, 4–6 samples of *Phragmites australis, Typha domingensis*, and *Potamogeton pectinatus* were collected from the lake shore and islets within a 5 m x 2 m plot. To remove sediments, roots and rhizomes were washed in the lake water and kept in plastic bags for transferring to the laboratory.

Fig. 2 **a** and **b** drainage waters from fishfarms that are distributed at the northern side of the Lake, **c** a canal which is located at the northern side to the Lake, **d** East El-Burullus area, **e** and **f** West El-Burullus Drain, **g** *Phragmites australis* species which is distributed nearby the connected area between El-Kashaa drain and the Lake, **h** and **i** *Typha domingensis* and *Eicchornia crassipes* species which were distributed along the shoreline and drain

Laboratory analyses

Water analysis

For the determination of heavy metals in water samples, the EPA digestion method was used according to Gregg (1989). A 100 ml of the representative water samples was put into Pyrex beakers containing 10 ml of concentrated HNO_3. The samples were slowly heated and then evaporated on a hot plate to the lowest possible volume (about 20 ml). The beakers were allowed to cool and another 5 ml of Conc. HNO_3 was added. The heating was continued with the addition of Conc. HNO_3 as necessary until digestion was completed. The samples were evaporated again to dryness (but not baked) and the beakers were cooled, followed by the addition of 5 ml of HCl solution (1:1 v/v). After warming the solutions, 5 ml of 5 M NaOH was added and then were filtered. The filtrates were transferred to 100 ml volumetric flasks and diluted to the mark with distilled water. These solutions were then used for the elemental analysis. A total of five metallic elements namely; Fe, Cu, Zn, Cd, and Pb were determined in the pre-treated samples of water using Atomic Absorption Spectrophotometry as described by Gregg (1989).

Sediment analysis

The concentration of heavy metals in sediments was determined according to EPA-ROC (1994). Where, conventional aqua regia digestion was prepared in glass beakers with volumes of 250 ml covered with watch glasses. A 0.5 g of sample was digested in 12 ml of aqua regia on a hotplate for three hours at 108 °C. After the evaporation process near drying, the samples were diluted with 20 ml HNO_3 of 2% (v/v with H_2O), then it was transferred into a 100 ml volumetric flask after filtering through Whatman No. 42 paper for dilution to 100 ml with double distilled water (DDW). Heavy metals (Fe, Cu, Zn, Cd and Pb) were analyzed using the atomic absorption spectrophotometer, and the results were expressed as microgram per gram (μg/g). Accuracy and precision were checked by using reference material (SD-M-2/IM).

Plant analysis

Plant samples were first dissected and divided into two parts above-ground and below-ground parts of plants; the first part (A) includes leaves and stems, and the second part (B) includes roots and rhizomes; to identify the various bioaccumulation capacities in the above-ground and below-ground parts. Plant organs were cut off using stainless steel scissors, and kept at 2 °C for further analysis. The sampled plants were rinsed thoroughly with distilled water, separated as mentioned before, dried at 70ºC for 72 h, crushed and digested using an acid mixture of concentrated H_2SO_4 and $HClO_4$ (Grimshaw 1987). The studied heavy metals (Fe, Cu, Zn, Cd and Pb) were determined using the flame atomic absorption spectrophotometer (FAAS, GBC-932), whereas data were expressed as μg/g.

Statistical analyses

Linear correlations between measured metals in the above-ground and below-ground parts of plants, water and sediments were tested through Pearson's r coefficient. The analysis of regression was also conducted. All statistical calculation and Polynomial regression analyses were performed using the software of PAST program.

After the analyses, the values were determined for bio-concentration or bio-accumulation and translocation factors to assess element mobility in the study species. The values obtained were based on the following:

$$\text{Bioaccumulation Factor (BAF)} = C_{\text{Plant part}}/C_{\text{medium}}$$

Where, $C_{\text{plant parts}}$ and C_{sediment} were the concentrations of metal ions in plant parts and medium (water and/or sediments) in μg/l and μg/g, respectively. BAF expresses the efficiency of plant species to accumulate metal ions from the surrounded medium. Higher BAF values imply a greater bioaccumulation capability (EPA 2007).

Landsat data treatment and analysis

Downloading satellite images and preprocessing

Downloading of a Landsat image from this site; https://earthexplorer.usgs.gov/ was done. The acquisition date is at 31/07/2021 close to the time of sampling collections. The radiometric corrections were occurred to convert it from digital numbers into reflectance using QGIS 3.16 program.

Analysis of Land Surface Temperature (LST) from Landsat images

Scientific theory of obtaining LST To obtain the LST, different steps should be considered;

I) Conversion of digital number into radiance

The use of Band 10 to recover the LST using ArcGIS 10.5 for digitizing the spectral radiance of B10 using the top of atmosphere (TOA) according to Barsi et al. (2014):

$$L\lambda = MLxQ_{Cal} + AL - O_i$$

Where; AL is the band-specific additive rescaling factor; ML is the band-specific multiplicative rescaling factor; Q_{cal} is the band 10 image; O_i is the band 10 correction.

II) Conversion to Maximum brightness temperature

The data of used band could be transformed into brightness temperature (BT) using the metadata file's thermal constant according to this equation;

$$TB = \frac{k_1}{\ln\left[\left(\frac{k_1}{L_\lambda}\right)\right] + 1} - 273.15$$

Where: K1, K2 = Bands Specific thermal conversion from the metadata; TB: Temperature of satellite brightness (Celsius); Emissivity correction is crucial to decreasing these inaccuracies and it was occurred to lastly obtain the LST from BT.

III) Land surface emissivity of NDVI (LSE)

The emissivity of the ground surface can be calculated using three equations based on the effectiveness of transporting thermal energy through the surface to the atmosphere. LSE is a proportionality factor that scales blackbody radiance (Planck's law) to predict emitted radiance according to the following equations; LSE is a proportionality coefficient that adjusts the radiance of the black body (Planck's law) to predict the emitted radiation.

$$\varepsilon_\lambda = \varepsilon_V Pv + \varepsilon_\lambda(1 - Pv) + d\varepsilon$$
$$d\varepsilon = (1 - \varepsilon_\delta)(1 - Pv)\, F\varepsilon_V$$
$$P_V = (NDVI_{Max} - NDVI_{Min})/(NDVI_{Max} + NDVI_{Min})$$
$$NDVI = \frac{NIR - RED}{NIR + RED}$$

Where ε_v: the vegetation emissivity, ε_s is the soil emissivity, P_v is the proportion of vegetation, F is a shape factor whose mean value is equal to 0.55, after assuming several geometrical distributions.

IV) Calculation of LST°C

Once, obtaining the emissivity images, the LST can be calculated using the following equation:

$$LST = \frac{BT}{1 + \frac{\lambda(BT) * \ln\epsilon}{\rho}}$$

Where: BT is the brightness temperature in Celsius (°C). LST is expressed in Celsius (°C). λ (11.5 μm) is the wavelength of emitted radiance: $\rho = h * c/\sigma = 1.438 * 10^{-2}$ mK, σ is the constant of Stefan–Boltzmann, ε is the land surface emissivity, c is the velocity of light, and h is Planck's constant, and (LSE) as described by Avdan and Jovanovska (2016). In the research, the methods are based on the online methodology for an image of summer season at 15 July 2021, respectively according to produced models of Parastatidis et al. (2017).

Calculations of remotely sensing indices

The remotely sensed indices which were represented the land cover were calculated as illustrated in Table 2.

Results

The extracted values of LST_s and land cover types' indices (NDVI, NDWI and NDMI) in a buffer of 100 m around the sampling plants were illustrated in Table 3 and Fig. 3. The average concentrations of heavy metals in both habitats of lake shores and islets of Lake Burullus were as follow; for the water of lake shores were; Fe > Pb > Zn > Cu > Cd; for the water around islets were; Fe > Zn > Pb > Cu > Cd. These orders in sediments take the following sequences; Fe > Zn > Cu > Pb > Cd in both the habitats. The average concentrations of metal ions in the above-ground parts of *Phragmites australis* were Fe > Zn > Pb > Cu > Cd in both. In the below-ground parts of *Phragmites australis*, this order was; Fe > Zn > Cu > Pb > Cd from the lake shore and Fe > Zn > Pb > Cu > Cd in the islets habitat. The concentrations of metal ions in the above parts of *Typha domingensis* in the lake shore were taken this sequence; Fe > Cu > Zn > Pb > Cd, in islets, this sequence was; Fe > Zn > Pb > Cu > Cd. Also these sequences were; Fe > Zn > Cu > Pb > Cd and Fe > Zn > Cu > Pb > Cd in the below-ground parts of *Typha domingensis* in both the habitats, respectively (Table 4). The raw concentrations of metal ions in water, sediments and plant species were illustrated in Appendix I.

The orders of average BAF_s in the studied area were as follow; Cd > Fe > Zn > Pb > Cu; Cd > Cu > Zn > Fe > Pb and Fe > Zn > Pb > Cu > Cd for *Typha domingensis, Phragmites australis* and *Potamogeton pectinatus* species, respectively as illustrated in Appendix II. The

Table 2 different remotely sensed indices in the study area

Index	Formula	Reference
Normalized difference water index	$NDWI = \frac{GREEN-NIR}{GREEN+NIR}$	(Xu 2006)
Normalized difference vegetation index	$NDVI = \frac{NIR-RED}{NIR+RED}$	(Leprieur et al. 2000)
Normalized difference moisture index	$NDMI = \frac{NIR-SWIR}{NIR+SWIR}$	(Gao 1995)

Table 3 The areas of land cover indices (in Km) in the studied buffers of 100 m around sampled plants within different sites

Stand	Site	Extracted LST	NDWI classes	Covered Km^2	NDVI classes	Covered Km^2	NDMI classes	Covered Km^2
1	Drain 7	30.00	No Water	0.030	No	0.000	MLCC	0.000
			Water	0.000	Sparse	0.006	ACC	0.013
					Moderate	0.014	MHCC	0.015
					High	0.008		
2	West Tirra	33.30	No Water	0.016	No	0.011	MLCC	0.000
			Water	0.016	Sparse	0.021	ACC	0.030
					Moderate	0.000	MHCC	0.001
					High	0.000		
3	El-Kashaa	--	No Water	0.000	No	0.030	MLCC	0.000
			Water	0.030	Sparse	0.000	ACC	0.030
					Moderate	0.000	MHCC	0.000
					High	0.000		
4	East El-Burullus	38.50	No Water	0.029	No	0.003	MLCC	0.022
			Water	0.003	Sparse	0.029	ACC	0.001
					Moderate	0.000	MHCC	0.008
					High	0.000		
5	El-Boughaz	30.83	No Water	0.008	No	0.007	MLCC	0.011
			Water	0.023	Sparse	0.024	ACC	0.021
					Moderate	0.000	MHCC	0.000
					High	0.000		
6	West El-Burullus	36.50	No Water	0.031	No	0.000	MLCC	0.002
			Water	0.000	Sparse	0.006	ACC	0.020
					Moderate	0.021	MHCC	0.009
					High	0.005		
7	El-Maksaba	25.50	No Water	0.023	No	0.008	MLCC	0.011
			Water	0.007	Sparse	0.023	ACC	0.020
					Moderate	0.000	MHCC	0.000
					High	0.000		
8	Brinbal	26.00	No Water	0.023	No	0.001	MLCC	0.004
			Water	0.003	Sparse	0.019	ACC	0.021
					Moderate	0.009	MHCC	0.005
					High	0.000		
9	El-Hoks	--	No Water	0.031	No	0.000	MLCC	0.003
			Water	0.000	Sparse	0.013	ACC	0.012
					Moderate	0.009	MHCC	0.015
					High	0.009		
10	El-Shaklouba	28.33	No Water	0.000	No	0.032	MLCC	0.000
			Water	0.032	Sparse	0.000	ACC	0.032
					Moderate	0.000	MHCC	0.000
					High	0.000		
11	El-Kome El-Akdar	30.43	No Water	0.025	No	0.004	MLCC	0.007
			Water	0.004	Sparse	0.022	ACC	0.023
					Moderate	0.004	MHCC	0.000
					High	0.000		
12	Besak	34.22	No Water	0.009	No	0.020	MLCC	0.000
			Water	0.022	Sparse	0.011	ACC	0.031
					Moderate	0.000	MHCC	0.000
					High	0.000		
13	El-Maktoaa	32.00	No Water	0.031	No	0.000	MLCC	0.000
			Water	0.000	Sparse	0.023	ACC	0.031
					Moderate	0.009	MHCC	0.000
					High	0.000		
14	Abu-Amer	32.00	No Water	0.019	No	0.011	MLCC	0.000
			Water	0.011	Sparse	0.008	ACC	0.017
					Moderate	0.01	MHCC	0.012
					High	0.000		

Table 3 (continued)

Stand	Site	Extracted LST	NDWI classes	Covered Km^2	NDVI classes	Covered Km^2	NDMI classes	Covered Km^2
15	Deshemy	29.00	No Water	0.021	No	0.006	MLCC	0.000
			Water	0.009	Sparse	0.016	ACC	0.012
					Moderate	0.009	MHCC	0.018
					High	0.000		

LST: land surface temperature, MLCC: mid-low canopy cover, ACC: average canopy cover and MHCC: mid-high canopy cover

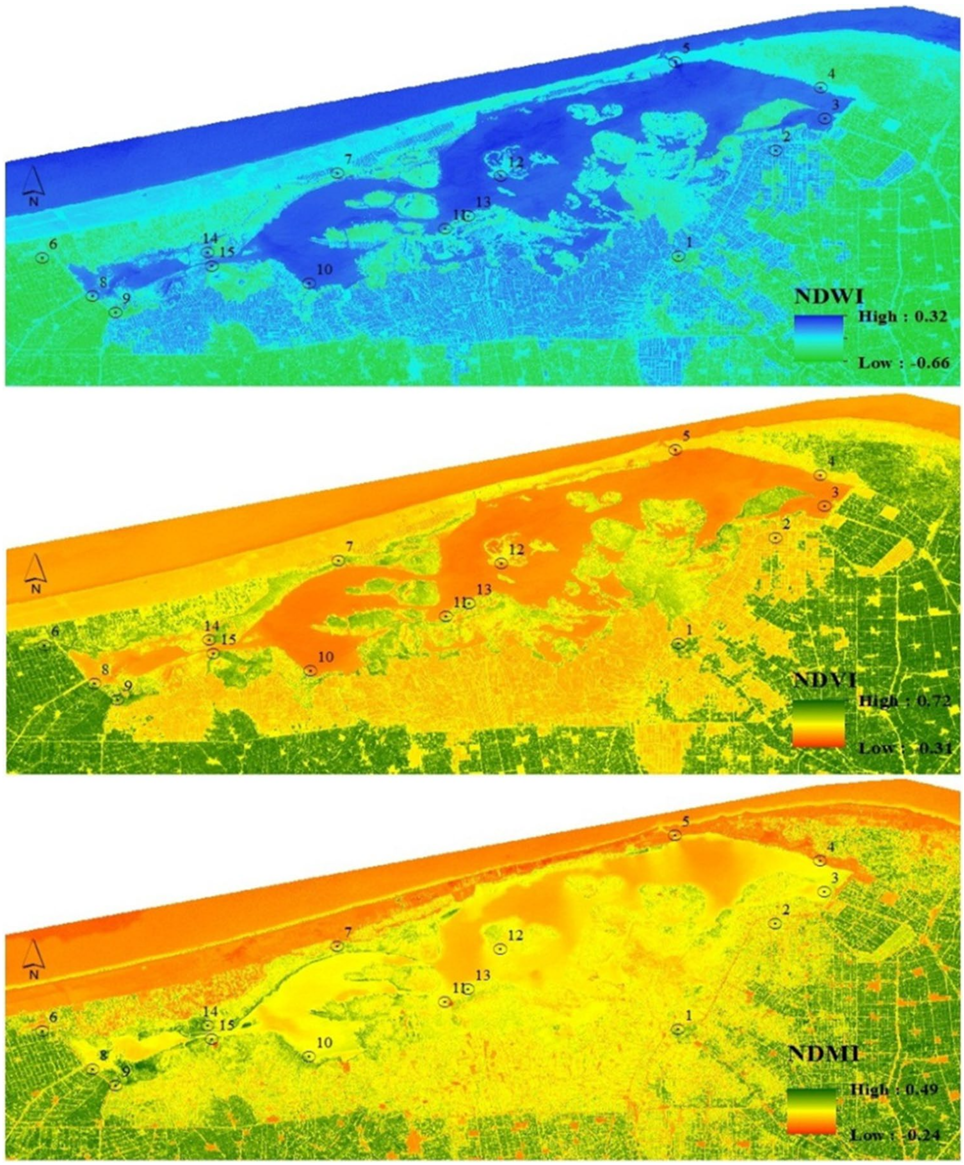

Fig. 3 NDWI, NDVI and NDMI along the studied area

Potamogeton pectinatus had BAFs values greater than one for Fe from its collected stands. Where the other values were lower than one for other metals except for Zn and Pb in one stand nearby Besak islet. But the other two species had BAFs lower than one for all metals.

The extracted values of LST in buffer areas of selected sites were ranged between 25.50 °C at El-Maksaba and 38.50 °C at East El-Burullus area. It was observed that *Potamogeton pectinatus* had the efficiency to accumulate

Table 4 Average concentrations of metals at water, sediment and three macrophytes at two studied ecological habitats of Burullus Lake

Habitat	Metal	Water µg/l	Sediment µg/g	*Phragmites australis* µg/g		*Typha domingensis* µg/g		*Potamogeton Pectinatus* µg/g (the whole plant)
				above	below	above	below	
Lake shores	Fe	182.8	25211.09	287.80	737.18	603.13	2674.09	-
	Cu	12.42	2333.50	5.90	5.84	41.56	19.15	-
	Zn	24.76	3056.48	33.61	20.93	35.01	93.42	-
	Cd	2.22	37.10	2.04	1.99	5.21	5.52	-
	Pb	29.27	2205.02	16.15	5.50	19.32	19.01	-
Islets	Fe	225.26	25449.27	200.82	824.37	230.56	529.83	-
	Cu	7.60	1842.69	4.53	4.45	4.28	4.15	-
	Zn	107.67	2700.75	71.38	25.76	39.15	16.85	-
	Cd	2.72	73.00	2.70	2.99	2.13	2.08	-
	Pb	27.96	873.00	10.85	9.55	7.45	10.45	-
Open Water	Fe	-	-	-	-	-	-	506.96
	Cu	-	-	-	-	-	-	3.90
	Zn	-	-	-	-	-	-	79.04
	Cd	-	-	-	-	-	-	1.82
	Pb	-	-	-	-	-	-	18.23

metal ions as Fe, Zn and Pb. Its BAF values were correlated positively with temperature.

From Fig. 4, it is obvious that the intake of Fe, Zn and Pb by *Potamogeton pectinatus* may be associated with the values of temperature as there is high significant correlation ($R^2 = 0.98$, 0.91 and 0.90), respectively. While, there was a highly negative significant correlation between low sparse vegetation (low vegetation cover) and the intake or accumulation of Pb. Other species of *Phragmites australis* and *Typha domingensis* showed low alterations with extracted LST_s values. There is also positive correlation with NDWI.

Results showed that some metals could be accumulated more in high vegetative habitats as Cd and Pb in the above parts of *Typha domingensis*. Whereas, other metals as Cu and Pb were accumulated in below parts of *Phragmites australis* in moderate vegetative areas. It was obtained that there were high positive significant correlation between the accumulation of Cu and Pb in below and above parts of *Phragmites australis* in moderate vegetative areas and mid-low canopy cover. In the above-ground parts of *Typha domingensis* species there were significant positive correlation between accumulation factor of Fe in moderate vegetation habitat and negatively with average canopy cover. While the accumulation of Cd and Pb increases in high vegetative locations. For below parts of *Typha domingensis*, results give indication that Zn accumulation decreases within low or sparse vegetation.

The regression analysis role was applied to obtain unknown information based on field studies (Austin 1971). The determination coefficient R^2 indicated that the most fitted regression models is for Fe with average canopy cover ACC and mid-high canopy cover MHCC habitats ($R^2 = 0.94$ and 0.92, respectively). For Pb, the regression analysis R^2 equal 0.77. In the above parts of *Phragmites australis*, the fitted polynomial regression was for Pb in conditions of high vegetative and mid to low canopy cover with R^2 equal to 0.77 and 0.93, respectively. Other models showed different significant ranged between low to moderate as illustrated in Fig. 5, 6, and 7; Table 5. Appendix III explained survey data of different vegetation of Burullus ecosystem.

Discussion

In the aquatic environments, the metal ions have been considered as a result of their toxicity, tendency to bio-concentrate and persistence. Nowadays, aquatic macrophytes were being used as functional intent for phytoremediation purposes. Recently, removal of metal ions from aqueous surface waters using accumulating roots and rhizomes (Pillai 2010; Xing et al. 2013).

The bioaccumulation factors are important to understand the availability of trace metals to plant species (Cheng 2003). Minerals content and compositions of plants differed significantly based on various species types (Kibar and Temel 2015). The ability of macrophytes to translocate and accumulate metal ions differs according to habitat species, tissues, prevailing climatic conditions, redox potential and pH (Eid et al. 2021). It was observed that the most accumulated element was Cd in *Typha domingensis* and *Phragmites australis*, while the most accumulated element ion in *Potamogeton*

Fig. 4 **A-E** The relation between BAF of metal ions in **A** *Potamogeton pectinatus*, **B** below-ground parts of *Phragmites australis*, **C** above-ground parts of *Phragmites australis*, **D** above-ground parts of *Typha domingensis* and **E** below-ground parts of *Typha domingensis* with land surface temperature and cover types' indices ▸

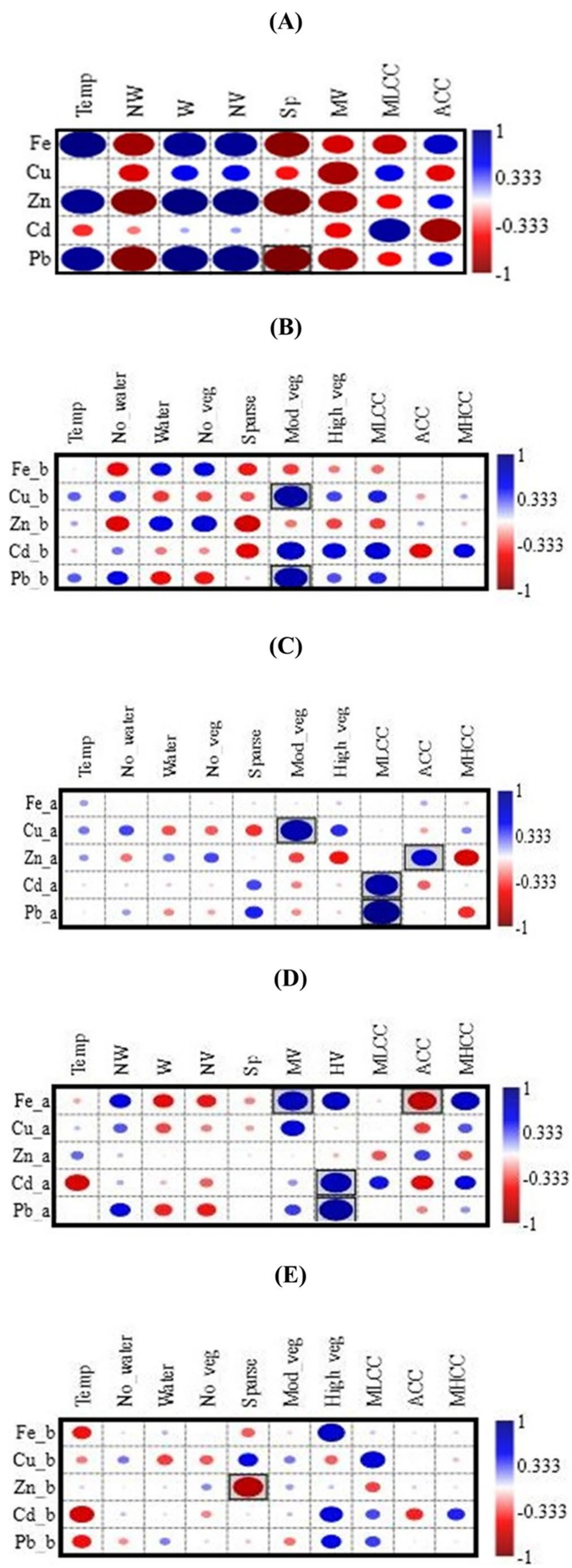

pectinatus was Fe. It was indication that *Typha domingensis* and *Phragmites australis* could be used as phytoremediated species to this toxic metal namely; Cd (Chandra and Yadav 2011; Mojiri et al. 2013; El-Amier et al. 2018) reported that the metal accumulation index (MAI) was more in *Phragmites australis* than *Typha domingensis* species. *Phragmites australis* may accumulate and translocate metal ions in shoot and root tissues. The BAF values are more than one in *Potamogeton pectinatus* that may cause toxic especially for Fe, Zn and Pb. While it mayn't any risk in case of other metals within the other species Majid et al. (2014).

Aquatic ecosystems were subjected to numerous stress factors; one of these is the increase in temperature due to climatic changes and metal disposal. So, thermal stress can magnify the impacts of metal ions on the aquatic macrophyes (Nin and Rodgher 2021). The LST is a significant indicator for the ecological and environmental changes in coastal wetlands and showed substantial spatiotemporal changes under severe sea-land interactions and different anthropogenic activities (Chi et al. 2020). The increase in sediment temperatures made influence on the vegetation mechanisms, metabolisms and the sediment characteristics itself, so it may enhance the sediment-plant translocations of metallic ions. So, the global temperature may effect on these pollutants bio-accumulation (Cornu et al. 2016; Lee and Kim 2022). The soil temperatures affected the capacity of different plant to accumulate metal ions such as; Cd, Zn, Cu and Pb. Principle component analysis proved that temperature, physiological and photosynthetic factors play role in the metal translocation properties of plant-soil (Yu et al. 2013).

The differences in LST_s of LULC types within different locations around or inside the lake area were clear. It may be interpreted as, saline basins and water areas caused lower LST, built-up areas and roads caused high LST, vegetative lands and islets caused medium LST, and barren areas possessed high LST (Chi et al. 2020). The correlation of BAF of *Potamogeton pectinatus* within temperature indicated the efficiency to accumulate metal ions. It is efficient to accumulate metals discharged in rainy waters at high temperature. *Potamogeton pectinatus* can accumulate more Zn (Fritioff et al. 2005).

Temperature showed low to no significance with BAF in *Phragmites australis* parts. There is low negative

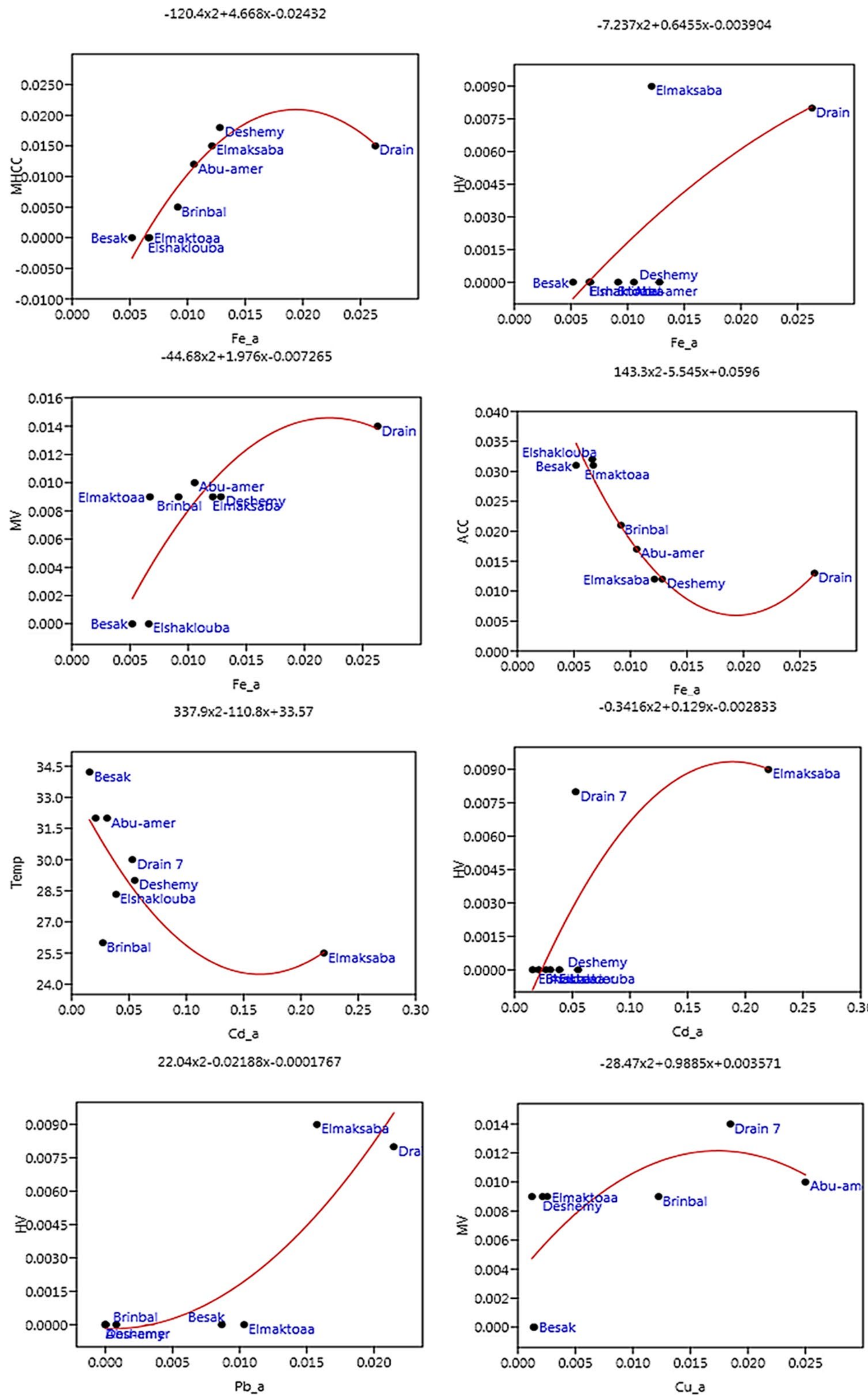

Fig. 5 Polynomial regression analysis between metal accumulation in the above-ground parts of *Typha domingensis* with LST and LC type in a buffer 100 m at Lake Burullus

significance correlation between above and below-ground parts of *Typha domingensis* and surface temperature for Cd. *Typha domingensis* has the ability to overcome the Cd toxicity and characterized by its potentiality of phytoremediation.

Vegetation Indices (VI_s) were insensitive indicators for monitoring the effects of metal in vegetation. As the spectrum alterations of leaf within different seasons may be caused by metal pollution (Zhou et al. 2018). The normalized difference moisture index (NDMI) explains the

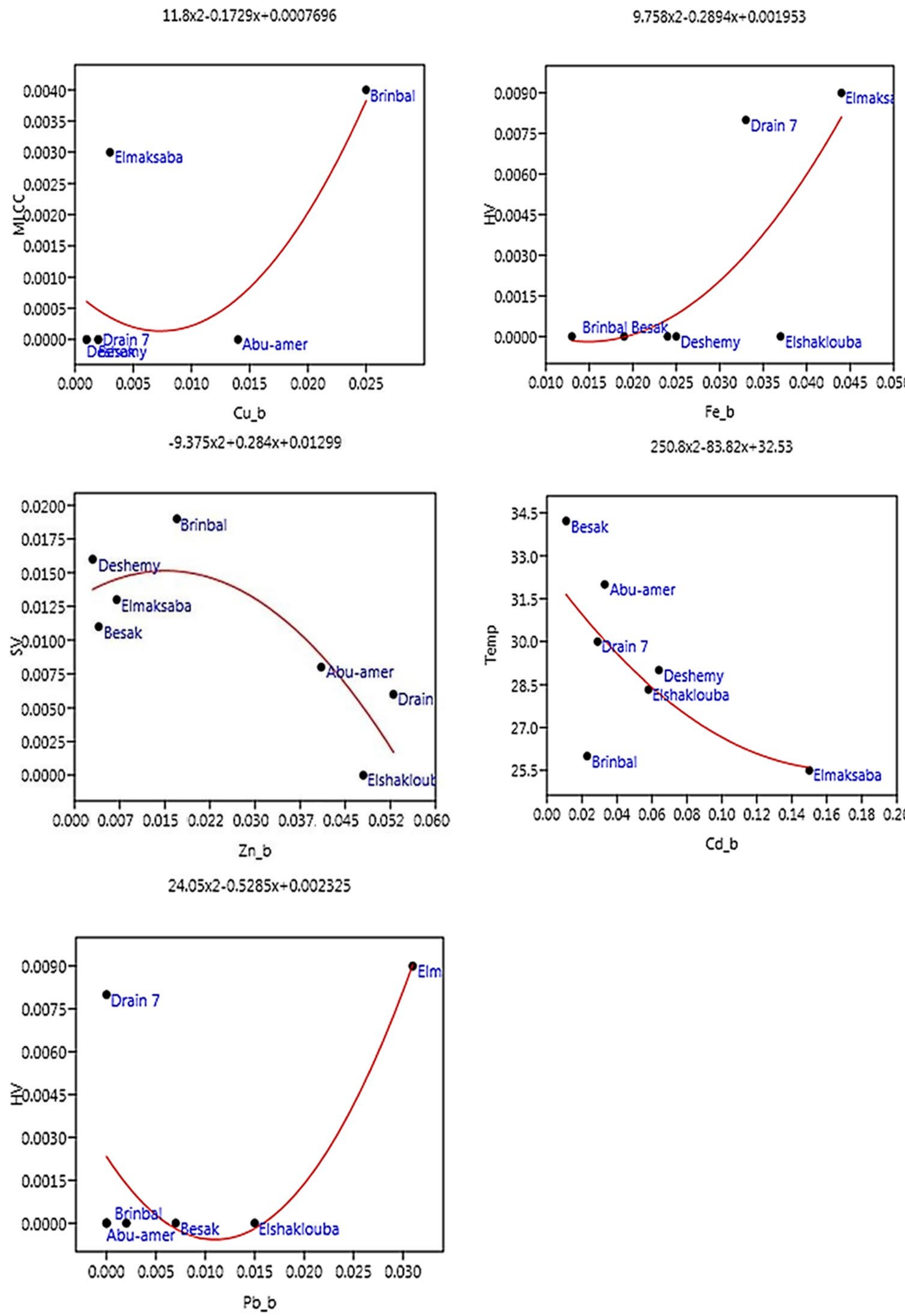

Fig. 6 Polynomial regression analysis between metal accumulation in the below-ground parts of *Typha domingensis* with LST and LC type in a buffer 100 m at Lake Burullus

vegetation content of water. It is suggested for monitoring moisture of vegetation using remote sensing data (Gao 1996). The vegetation water content considers one of the vital biophysical characteristics of the healthy vegetation. The NDWI can aid in the evaluation of dryness stress on the aquatic vegetation of Mediterranean type ecosystems through plant available water (Serrano et al. 2019). The moisture content was also known as a function of plant sample's water content (Makarius et al. 2013). It could be used for monitoring the water stress in vegetation (Zhang et al. 2019). It is obvious that canopy water content is a comprehensive indicator reflecting the vigor and health of vegetation growth. Vegetation water content is one of the significant biophysical of vegetation health features, and its remote valuation can be exploited to real-timely monitor vegetation water stress. It can be used to different factors as

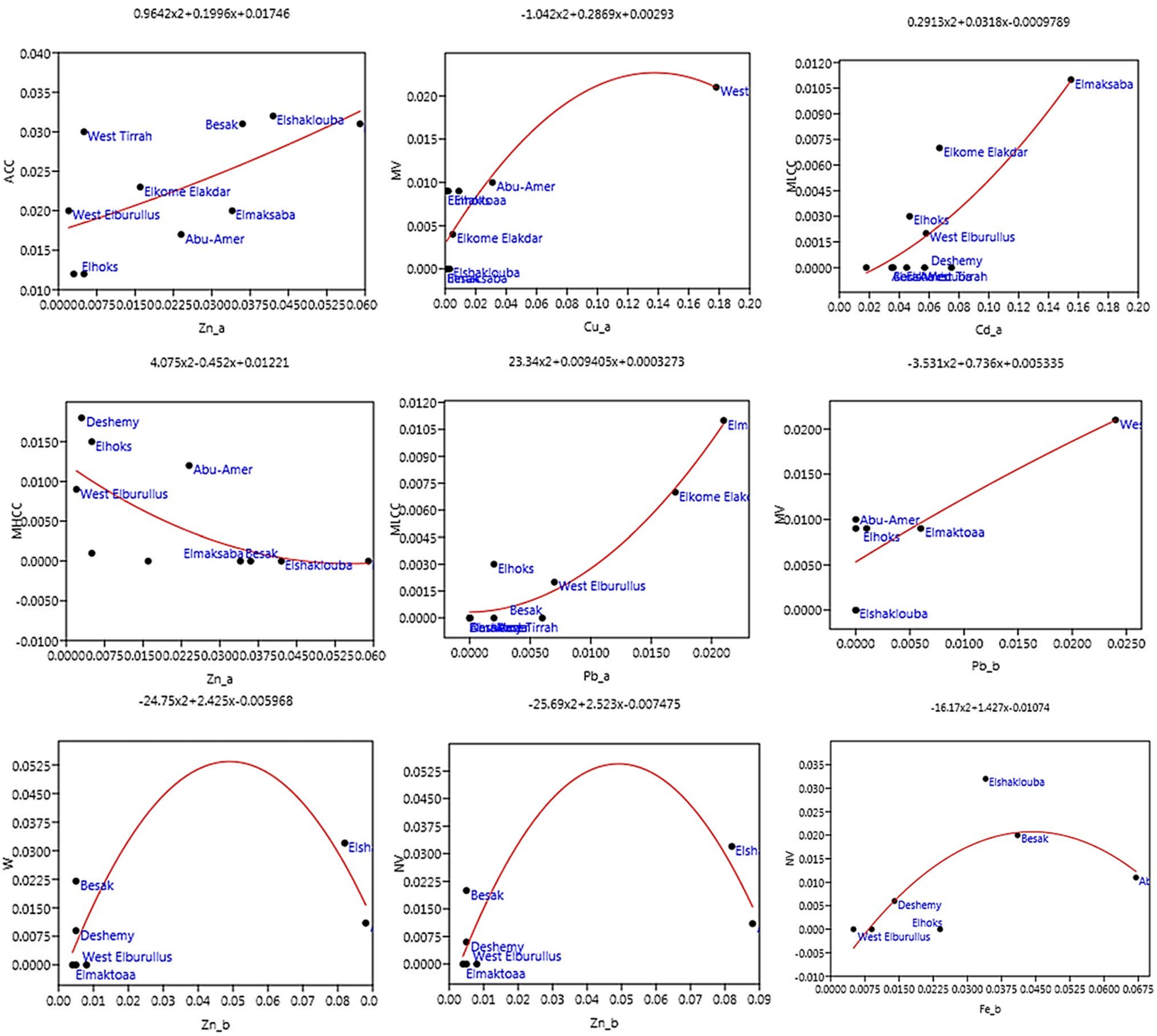

Fig. 7 Polynomial regression analysis between metal accumulation in the above and below ground parts of *Phragmites australis* with LST and LC type in a buffer 100 m at Lake Burullus

canopy water content for further water treatments (Zhang and Zhou 2019). It was may be interpreted that it had the ability to adsorb more metals and efficiency of water stress treatment increase. This was especially for Fe in the above-ground parts of *Typha domingensis* and Zn in the above-ground parts of *Phragmites australis*. Also, the water content of the plant shoots in below-ground parts in water habitats of low minerals content than those of high nutrients (Drew 1967). The vigor NDVI not only represented by the dense of habitat; as some metals may cause change in NDVI. For example, high concentrations of Zn in plant species may induce significant decreases in NDVI (Chen et al. 2009). It was clear from the correlations in this study.

It is clear that the abundance of watered habitats was vital for the submerged vegetation as *Potamogeton pectinatus*. It is obvious that the accumulation of Fe, Zn and Pb increases in water conditions, whereas the accumulation of Cu and Cd can occur with low water conditions. While NDWI represented low to no significant correlation with other two species.

Using multiple regressions in prediction process is a tool used to forecast dependent factors from a group of

Table 5 The polynomial regression model between accumulated metals in above and below-ground parts of plants with different land cover indices from satellite image

Plant species	Metal	Index	Polynomial regression models	R^2
Above-ground Parts of *Typha domingensis*	Fe	MV	$-44.68\times^2+1.976x-0.0073$	0.68
		HV	$-7.23\times^2+0.645x-0.003$	0.49
		ACC	$143.3\times^2-5.545x+0.059$	0.94
		MHCC	$-120.4\times^2+4.668x-0.024$	0.92
	Cd	Temp	$337.9\times^2-110.8x+33.57$	0.45
		HV	$-0.341\times^2+0.129x-0.0028$	0.63
	Pb	HV	$22.04\times^2-0.0218x-0.00017$	0.77
	Cu	MV	$-28.47\times^2-0.988x+0.0035$	0.43
Below-ground Parts of *Typha domingensis*	Fe	HV	$9.75\times^2-0.289x+0.001$	0.53
	Cu	MLCC	$11.8\times^2-0.172x+0.00076$	0.52
	Zn	SP	$-9.37\times^2+0.28x+0.012$	0.69
	Pb	HV	$24.05\times^2-0.528x+0.0023$	0.56
	Cd	HV	$250.8\times^2-83.82x+32.53$	0.46
Above-ground Parts of *Phragmites australis*	Cu	MV	$-1.042\times^2+0.286x+0.002$	0.70
	Zn	ACC	$0.96\times^2-0.199x+0.017$	0.40
		MHCC	$4.075\times^2-0.45x+0.0122$	0.42
	Cd	MLCC	$0.29\times^2+0.0318x-0.00097$	0.70
	Pb	MLCC	$23.34\times^2+0.0094x+0.0003$	0.93
Below-ground Parts of *Phragmites australis*	Fe	NV	$-16.17\times^2+1.42x-0.01$	0.57
	Zn	W	$-24.75\times^2+2.42x-0.0059$	0.51
		NV	$-25.69\times^2+2.52x-0.007$	0.44
	Pb	MV	$-3.531\times^2-0.736x+0.0053$	0.66

independent factors (Eid et al. 2010a, b). Also regression models were suitable to predict metal accumulation in plants and more useful when being compared with numerous validation tools (Kumar et al. 2020). The coefficient factor (R^2) is important in the prediction models. Abd El-Hamid et al. (2022) stated that R^2 and root mean squares errors RMSE were fit to evaluate the accuracy of these models. It is observed from results that the most fitted models are for Fe with ACC and MHCC; and Pb with MLCC in the above-ground parts of *Typha domingensis* and *Phragmites australis*, respectively.

Conclusion

The study involved land use/cover of fifteen habitats within and around Lake Burullus. The integration of different remote sensing indices was aided more in identifying the differences in plant efficiencies of metal accumulation. Each plant species can accumulate different metals within different LST, NDVI, NDWI and NDMI values. Polynomial regression models were aided in the prediction of metal accumulators within different habitats in the case of integration of remotely sensed indices. Extracted surface temperatures showed more influences with the submerged species as *Potamogeton pectinatus* more than those of *Phragmites australis* and *Typha domingensis*. NDVI values may be interpreted in different two trends; one is the vegetation health and or the dense presence and distribution in the ecosystem. *Potamogeton* showed high accumulation within water conditions. The two species of *Phragmites australis* and *Typha domingensis* has the ability to accumulate metal ions in different habitats more than Potamogeton. This is an indication to the availability to grow and endure in polluted habitats. So these macrophytes species were highly recommended to be used for the remediation of polluted waters by metals in similar habitats' conditions.

Appendix

I) Raw data of metal ions in water (μg/L), sediment and plants (μg/G)

No	Medium	Fe	Cu	Zn	Cd	Pb
Drain 7	A) Water	393.30	16.00	27.30	3.90	39.70
El-Maktoaa		85.10	18.60	42.90	6.50	61.70
Brinbal		33.10	13.20	29.30	3.30	39.10
El-Kashaa		63.40	9.70	24.40	1.10	16.40
Ebsak		43.40	10.60	16.70	4.20	30.20
El-Maksaba		90.60	14.30	42.40	3.10	35.00
West Tirrah		25.80	8.10	21.90	1.40	22.80
West El-Burullus		8.00	10.20	55.20	0.60	3.90
El-Bughaz		285.00	15.70	4.60	5.80	44.50
El-Kome El-Akdar		164.30	2.60	52.60	2.90	47.90
East El-Burullus		72.00	19.30	19.20	2.10	59.00
El-Hoks		12.40	13.80	9.60	ND	32.30
Abu-Amer		132.30	4.70	395.53	ND	ND
Deshemy		701.20	1.50	30.60	ND	ND
El-Shaklouba		844.40	3.90	13.70	0.90	ND
West El-Burullus	B) Sediment	25295.08	36.00	2807.55	31.00	1013.00
El-Maksaba		24315.53	1842.00	1790.00	10.00	495.00
El-Hoks		26229.93	746.00	4550.59	31.00	6505.49
Besak		25827.68	3384.48	3048.00	131.00	1598.00
El-Maktoaa		26542.79	1529.00	3425.69	103.00	1544.00
East El-Burullus		21812.65	3348.57	874.00	7.00	572.00
El-Boughaz		25201.96	156.00	4568.48	21.00	4510.23
Drain 7		26542.79	6724.28	3737.44	34.00	943.00
West Tirrah		26578.17	3874.11	3644.85	34.00	894.00
El-Kashaa		25466.41	3451.05	3070.55	71.00	1149.00
El-Kome El-Akdar		22624.60	1562.00	1048.00	23.00	750.00
Brinbal		25563.24	376.00	4866.36	92.00	5827.46
Abu-Amer		26157.30	110.00	481.00	68.00	434.00
Deshemy		26093.99	2628.00	5501.05	40.00	39.00
El-Shaklouba		25105.13	2781.00	655.00	40.00	141.00

C) Plant species	Part	Site	Fe	Cu	Zn	Cd	Pb
Typha domingensis	Above	Drain 7	697.70	124.20	31.40	1.80	20.25
Typha domingensis	Below	Brinbal	478.60	9.45	82.10	2.10	9.35
Phragmites australis	Above	El-Maksaba	287.80	4.25	61.75	1.55	10.55
Typha domingensis	Below	El-Maksaba	1069.78	5.40	13.35	1.50	15.55
Phragmites australis	Below	El-Hoks	628.05	7.65	17.90	2.25	4.95
Typha domingensis	Below	El-Kashaa	10020.13	66.22	143.24	20.72	68.47
Phragmites australis	Below	El-kmoe El-Akdar	864.18	10.00	22.55	1.75	16.05
Phragmites australis	Below	West El-Burulls	621.16	6.40	5.85	1.80	7.25
Typha domingensis	Above	Brinbal	234.15	4.60	9.10	2.50	4.65
Typha domingensis	Above	Besak	134.00	4.80	12.90	2.05	13.85
Phragmites australis	Above	Elkome El-Akdar	278.00	7.70	16.65	1.55	12.45
Phragmites australis	Below	El-Maktoaa	133.40	1.45	17.40	1.95	9.55

C) Plant species	Part	Site	Fe	Cu	Zn	Cd	Pb
Potamogeton Pectinatus	-	Elkome El-Akdar	555.79	1.70	12.10	2.05	10.25
Potamogeton Pectinatus	-	El-Maktoaa	471.60	3.65	22.05	1.45	12.85
Phragmites australis	Below	Elkome El-Akdar	196.75	4.65	15.65	2.25	6.05
Phragmites australis	Above	El-Maktoaa	179.55	3.20	200.97	1.90	ND
Phragmites australis	Below	West Tirra	851.70	4.45	18.60	1.95	2.00
Typha domingensis	Below	Besak	615.66	7.35	13.50	1.45	10.45
Typha domingensis	Above	El-Kashaa	1622.97	72.97	99.10	18.02	44.59
Typha domingensis	Above	El-Maksaba	294.80	2.25	23.20	2.20	7.80
Phragmites australis	Below	Elkome El-Akdar	768.65	4.15	23.75	1.95	2.90
Phragmites australis	Above	El-Hoks	269.40	6.40	22.50	1.45	13.90
Typha domingensis	Above	El-Maktoaa	178.00	3.90	121.60	2.15	15.95
Phragmites australis	Above	West El-Burullus	221.20	5.35	22.75	3.35	24.00
Phragmites australis	Below	Besak	1048.55	5.85	15.00	3.20	ND
Typha domingensis	Below	Drain 7	884.11	11.85	196.67	1.00	ND
Potamogeton pectinatus	-	Besak	493.50	6.35	202.98	1.95	31.60
Phragmites australis	Above	Besak	167.20	4.65	110.20	4.70	9.25
Typha domingensis	Above	Abu-Amer	276.15	2.75	12.20	2.10	ND
Typha domingensis	Below	Abu-Amer	334.15	1.55	19.55	2.25	ND
Phragmites australis	Above	Abu-Amer	11.95	3.40	11.55	2.35	ND
Phragmites australis	Below	Abu-Amer	1755.49	3.89	42.22	4.67	ND
Typha domingensis	Above	Deshemy	334.10	5.65	9.90	2.20	ND
Typha domingensis	Below	Deshemy	639.69	3.55	17.50	2.55	ND
Phragmites australis	Above	Deshemy	367.40	3.70	17.55	3.00	ND
Phragmites australis	Below	Deshemy	360.05	6.60	28.40	2.15	ND
Typha domingensis	Above	El-Shaklouba	166.05	3.80	12.25	1.55	ND
Typha domingensis	Below	El-Shaklouba	917.8148	2.85	31.75	2.3	2.15
Phragmites australis	Above	El-Shaklouba	362.05	7.6	27.45	1.8	ND
Phragmites australis	Below	El-Shaklouba	854.6842	6.1	53.4	2.4	ND

II) Bioaccumulation factor values in different parts of plant species

Site	Selected Species	Part	BAF				
			Fe	Cu	Zn	Cd	Pb
Drain 7	*Typha domingensis*	A	0.026	0.018	0.008	0.053	0.021
Drain 7	*Typha domingensis*	B	0.033	0.002	0.053	0.029	0.000
Brinbal	*Typha domingensis*	B	0.019	0.025	0.017	0.023	0.002
Brinbal	*Typha domingensis*	A	0.009	0.012	0.002	0.027	0.001
El-Maksaba	*Phragmites australis*	A	0.012	0.002	0.034	0.155	0.021
El-Maksaba	*Typha domingensis*	A	0.012	0.001	0.013	0.220	0.016
El-Maksaba	*Typha domingensis*	B	0.044	0.003	0.007	0.150	0.031
El-Hoks	*Phragmites australis*	A	0.010	0.009	0.005	0.047	0.002
El-Hoks	*Phragmites australis*	B	0.024	0.010	0.004	0.073	0.001
El-Kashaa	*Typha domingensis*	B	0.393	0.019	0.047	0.292	0.060
West El-Burulls	*Phragmites australis*	B	0.025	0.178	0.002	0.058	0.007
Besak	*Typha domingensis*	A	0.005	0.001	0.004	0.016	0.009
Besak	*Typha domingensis*	B	0.024	0.002	0.004	0.011	0.007
El-Kome El-Akdar	*Phragmites australis*	A	0.012	0.005	0.016	0.067	0.017
El-Maktoaa	*Phragmites australis*	B	0.005	0.001	0.005	0.019	0.006
El-Maktoaa	*Phragmites australis*	A	0.007	0.002	0.059	0.018	0.000
El-Maktoaa	*Typha domingensis*	A	0.007	0.003	0.035	0.021	0.010

Site	Selected Species	Part	BAF				
			Fe	Cu	Zn	Cd	Pb
El-Maktoaa	*Potamogeton pectinatus*	-	5.542	0.196	0.514	0.223	0.208
El-Kkome El-Akdar	*Potamogeton pectinatus*	-	3.383	0.654	0.230	0.707	0.214
Besak	*Phragmites australis*	A	0.006	0.001	0.036	0.036	0.006
Besak	*Phragmites australis*	B	0.041	0.002	0.005	0.024	0.000
Besak	*Potamogeton pectinatus*	-	11.371	0.599	12.154	0.464	1.046
West Tirrah	*Phragmites australis*	B	0.032	0.001	0.005	0.057	0.002
El-Kashaa	*Typha domingensis*	A	0.064	0.021	0.032	0.254	0.039
West El-Burullus	*Phragmites australis*	A	0.009	0.149	0.008	0.108	0.024
Abu_Amer	*Typha domingensis*	A	0.011	0.025	0.025	0.031	0.000
Abu_Amer	*Typha domingensis*	B	0.013	0.014	0.041	0.033	0.000
Abu_Amer	*Phragmites australis*	A	0.000	0.031	0.024	0.035	0.000
Abu_Amer	*Phragmites australis*	B	0.067	0.035	0.088	0.069	0.000
Deshemy	*Typha domingensis*	A	0.013	0.002	0.002	0.055	0.000
Deshemy	*Typha domingensis*	B	0.025	0.001	0.003	0.064	0.000
Deshemy	*Phragmites australis*	A	0.014	0.001	0.003	0.075	0.000
Deshemy	*Phragmites australis*	B	0.014	0.003	0.005	0.054	0.000
El-Shaklouba	*Typha domingensis*	A	0.007	0.001	0.019	0.039	0.000
El-Shaklouba	*Typha domingensis*	B	0.037	0.001	0.048	0.058	0.015
El-Shaklouba	*Phragmites australis*	A	0.014	0.003	0.042	0.045	0.000
El-Shaklouba	*Phragmites australis*	B	0.034	0.002	0.082	0.060	0.000

A: Above-ground and B: Below-ground

III) Data survey of different plant species along the Lake Shoreline and islets of Lake Burullus

A) Hydrophytes		Presence in study area	Life Span
1- Floating hydrophytes			
	Eicchornia crassipes C. Mart.	Drain 7, West El-Burullus, El-Hoks, Deshemy	Per
2- Submerged hydrophytes			
	Potamogeton pectinatus L.	Brinbal, Deshemy, El-Maktoaa, El-Kome El-Akdar	Ann
3- Emergent species			
	Phragmites australis Cav.	All Sites	Per
	Typha domingensis Pers.	El-Kashaa, Drain 7, West El-Burullus, El-Maksaba, El-Hoks, Abu-Amer, Deshemy, El-Shaklouba, Besak, El-kome El-Akdar, El-Maktoaa	Per
	Echinochloa stagnina Retz.	Drain 7, East El-Burullus, West El-Burullus, Brinbal, El-Hoks	Per
B) Terrestrial species			
	Bassia indica Wight	Tirra, East El-Burullus, Brinbal,	Ann
	Cynanchum acutum L.	Hawis, Tirra, East El-Burullus, Brinbal, Abu-Amer, Deshemy	Per
	Juncus rigidus Desf.	Deshemy,	Per
	Suaeda pruinosa Lange	El-Kashaa, El-Maksba	Per
	Alhagi graecorum Boiss.	Drain 7	Per
	Arthrocnemum macrostachyum Moric.	Drain 7, El-Maksba, Deshemy	Per
	Atriplex canescens	West El-Burullus, Deshemy	Per
	Aster aqumatus	Tirra, Brinbal,	Per
	Rumex dentatus	Tirra,	Per
	Pluchea dioscorides L.	El-Kashaa, East El-Burullus, Brinbal, El-Hoks	Per
	Tamarix nilotica Ehrenb.	El-Kashaa, East El-Burullus	Per
Number of perennials			14
Number of annuals			2
Total number of recorded species			16

Acknowledgements Authors acknowledge Prof. Mahmoud Dar, Dr. Mohamed Metwally and Dr. Amany Madkur, National Institute of Oceanography and Fisheries, NIOF, Egypt; for their aid in measuring and calculation of metal ions. Also authors want to thank Mr. Mohamed Abdullah Amer, Faculty of Science, Al-Azhar University, Egypt; for the aid in samples' analyses.

Author contributions The point of this research is suggested and designed by MAE and MSS. MAE, MSS and AIB collected samples and field survey. MAE, AIB and DHD analyzed samples. MAE, MF and DHD wrote the first draft. All authors wrote and revised the final draft of Manuscript. All authors approved the version of manuscript.

Funding Open access funding provided by The Science, Technology & Innovation Funding Authority (STDF) in cooperation with The Egyptian Knowledge Bank (EKB).

Data availability All data generated during the research are included in this original paper.

Declarations

Consent to participate Not applicable.

Consent for publication Not applicable.

Conflict of interest Authors declare no conflict of interest.

References

Abd El-Hamid HT, Rabie R, Zarzoura F, Hafiz MA, El-Alfy MA (2022) Integrated approach of remote sensing and machine learning to simulate and predict petroleum pollution and algal blooms along Aqaba Gulf. Biocatal Agric Biotechnol 46:102528

Abd el-sadek E, Elbeih S, Negm A (2022) Coastal and land use changes of Burullus Lake, Egypt: a comparison using landsat and Sentinel-2 satellite images. Egypt J Remote Sens Space Sci 25(3):815–829

Abdel-Ghani NT, Hegazy AK, El-Cheghaby GA, Lima EC (2009) Factorial experimental design for bio-sorption of iron and zinc using *Typha domingensis* phytomass. Desalination 249(1):343–347

Avdan U, Jovanovska G (2016) Algorithm for automated mapping of land surface temperature using LANDSAT 8 satellite data. J Sensors 2016:1480307

Al-Yemni MN, Sher H, El-Sheikh MA, Eid EM (2011) Bioaccumulation of nutrient and heavy metals by Calotropis procera and Citrullus colocynthis and their potential use as contamination indicators. Sci Res Essays 6(4):966–976

Amini Ranjbar GH (1998) Heavy metal concentration in surficial sediments from Anzali Wetland, Iran. Water Air Soil Pollut 104(3/4):305–312

Austin MP (1971) Role of regression analysis in ecology. In: Quantifying Ecology. The Proceedings of the Ecological Society of Australia 6: 63–75

Balah MI (2012) North Delta Lakes, Egypt. In: Encyclopedia of Lakes and Reservoirs; Encyclopedia of Earth Sciences Series. Springer, Dordrecht, pp 562–578

Baldantoni D, Ligrone R, Alfani A (2009) Macroand trace-element concentrations in leaves and roots of Phragmites australis in a volcanic lake in Southern Italy. J Geochem Explor 101(2):166–174

Bargagli R (1998) Trace elements in terrestrial plants. An ecophysiological approach to biomonitoring and biorecovery. Springer, Berlin, p 324

Barsi JA, Schott JR, Hook SJ, Raqueno NG, Markham BL, Radocinski RG (2014) Landsat-8 thermal infrared sensor (TIRS) vicarious radiometric calibration. Remote Sens 6:11607–11626. https://doi.org/10.3390/rs61111607

Barwick M, Maher W (2003) Biotransference and biomagnification of selenium, copper, cadmium, zinc, arsenic and lead in a temperate seagrass ecosystem from Lake Macquarie Estuary, NSW, Australia. Mar Environ Res 56:471–502

Bonanno G (2011) Trace element accumulation and distribution in the organs of Phragmites australis (common reed) and biomonitoring applications. Ecotoxicol Environ Saf 74(4):1057–1064

Bonanno G, Giudice RL (2010) Heavy metal bioaccumulation by the organs of Phragmites australis (common reed) and their potential use as contamination indicators. Ecol Ind 10(3):639–645

Bornete G, Puijalon S (2011) Response of aquatc plants to abiotc factors: a review. Aquatc Sci 73:1–14

Boulos L (2005) Flora of Egypt. In: Monocotyledons (*Altismataceae – rchidaceae*),, vo. 4. Al-Hadara Publishing, Cairo, p 617

Casagranda C, Boudouresque CF (2007) Biomass of Ruppia cirrhosa and Potamogeton pectinatus in a Mediterranean brackish lagoon, Lake Ichkeul, Tunisia. Fundam Appl Limnol 168:243–255

Chandra R, Yadav S (2011) Phytoremediation of CD, CR, CU, MN, FE, NI, PB and ZN from aqueous solution using *Phragmites Cummunis*, *Typha Angustifolia* and *Cyperus Esculentus* Int J Phytoremediation 13(6):580–591. https://doi.org/10.1080/15226514.2010.495258

Chen J, Shi ZQ, Hu LB, Su Y, Han FX, Monts DL (2009) Site assessment, long-term monitoring and regulatory concerns for application of phytoremediation technology for remediation of heavy metal/metalloid - contaminated soils. In: Solid Waste Management and Environmental Remediation, pp 407–421

Cheng S (2003) Heavy metals in plants and phytoremediation. Environ Sci Pollut Res 10:335

Chi Y, Sun J, Sun Y, Liu S, Fu Z (2020) Multi-temporal characterization of land surface temperature and its relationships with normalized difference vegetation index and soil moisture content in the Yellow River Delta, China. Global Ecol Conserv 23:e01092

Clayton WD, Vorontsova MS, Harman KT, Williamson H (2006) GrassBase - The Online World Grass Flora. Available:http://www.kew.org/data/grasses-db.htm. Accessed 8 Nov 2006

Cornu J, Denaix L, Lacoste J, Nguyen C (2016) Impact of temperature on the dynamics of organic matter and on the soil-to-plant transfer of cd, zn and pb in a contaminated agricultural soil. Environ Sci Pollut Res 23(4):2997–3007. https://doi.org/10.1007/s11356-015-5432-4

Dar SA, Bhat SU, Rashid I (2021a) The status of current knowledge, distribution, and conservation challenges of wetland ecosystems in Kashmir Himalaya, India. Current Challenges and Future Strategies, Wetlands Conservation, pp 175–200

Dar SA, Bhat SU, Rashid I (2021b) Landscape transformations, morphometry, and trophic status of Anchar Wetland in Kashmir Himalaya: implications for urban wetland management. Water Air Soil Pollut 232:1–19. https://doi.org/10.1007/s11270-021-05416-5

Dar SA, Bhat SU, Rashid I, Kumar P, Sharma R, Aneaus S (2022a) Deciphering the source contribution of organic matter accumulation in an urban wetland ecosystem. Land Degrad Dev 33(13):2390–2404. https://doi.org/10.1002/ldr.4280

Dar SA, Hamid A, Rashid I, Bhat SU (2022b) Identification of anthropogenic contribution to wetland degradation: insights from the environmetric techniques. Stoch Env Res Risk Assess 36:1397–1411. https://doi.org/10.1007/s00477-021-02121-x

Dar SA, Lone FA, Dar SA, Bhat RA, Bashir I, Mir SA, Dar ZA (2020) Biofilm: an innovative modern technology for aquatic pollution remediation. Bioremediat Biotechnol 2:207–219

Drew DH (1967) Mineral nutrition and the water relations of plants i. A comparison of the effects of mineral-free w'ater and nutrient solutions on water uptake and transpiration. Plant Soil 26:158–174

Duke JA (1978) The quest for tolerant germplasm. In: ASA Special Symposium 32, Crop Tolerance to Suboptimal Land Conditions. American Society of Agronomy. Madison, pp 1–61

Duke JA (1979) Ecosystematic data on economic plants. Q J Crude Drug Res 17(3–4):91–110

Eid EM (2012) *Phragmites australis* (Cav.) Trin. ex Steud.: its popLAMulation biology and nutrient cycle in Lake Burullus, a Ramsar site in Egypt. LAP BERT Academic Publishing, Saarbrücken

Eid EM, Shaltout KH, Al-Sodany YM, Jensen K (2010a) Efects of abiotic conditions on Phragmites australis along geographic gradients in lake Burullus, Egypt. Aquat Bot 92(2):86–92. https://doi.org/10.1016/j.aquabot.2009.10.010

Eid EM, Shaltout KH, Al-Sodany YM, Soetaert K, Jensen K (2010b) Modeling growth, carbon allocation and nutrient budget of Phragmites australis in Lake Burullus, Egypt. Wetlands 30(2):240–251

Eid EM, Shaltout KH, Asaeda T (2012) Modeling growth dynamics of *Typha domingensis* (Pers.) Poir. ex Steud. in Lake Burullus, Egypt. Ecol Modell 243:63–72

Eid EM, Shaltout KH, Almuqrin AH, Aloraini DA, Khedher KM, Taher MA, Alfarhan AH, Picó Y, Barcelo D (2021) Uptake prediction of nine heavy metals by Eichhornia crassipes grown in irrigation canals: A biomonitoring approach. Science of The Total Environment 782:146887

El Garouani M, Amyay M, Lahrach A, Oulidi HJ (2021) Land surface temperature in response to land use/cover change based on remote Sensing data and GIS techniques: application to Saïss Plain, Morocco. J Ecol Eng 22(7):100–112. https://doi.org/10.12911/22998993/139065

El-Amier YA, El-Alfy MA, Nofal MM (2018) Macrophytes potential for removal of heavy metals from aquatic ecosystem, Egypt: using metal accumulation index (MAI). Plant Arch 18(2):2131–2144

El-Shinnawy I (2002) Al-Burullus wetland's hydrological study. Med wet coast, Global Environmental Facility (GEF) and Egyptian Environmental Affairs Agency (EEAA), Cairo

EPA (2007) Framework for metal risk assessment. U.S Environmental Protection Agency. Office of the Science Advisor, Washington DC

EPA ROC, Taipei (1994) The standard methods for determination of heavy metals in soils and plants. National Institute of Environmental Analysis of EPA-ROC, Taiwan (In Chinese)

Fritioff A, Kautsky L, Greger M (2005) Influence of temperature and salinity on heavy metal uptake by submersed plants. Environ Pollut 133:265–274

Gao B (1995) Normalized difference water index for remote sensing of vegetation liquid water from space. SPIE Conf Proc 2480:225–236. https://doi.org/10.1117/12.210877

Gao B (1996) NDWI—A normalized difference water index for remote sensing of vegetation liquid water from space. Remote Sens Environ 58(3):257–266

Gregg LW (1989) Water analysis Handbook. H.A.C.H Company, USA, pp 33–39

Grimshaw HM (1987) The determination of total phosphorus in soils by acid digestion. In: Rowland AP (ed) Chemical analysis in environmental research. Abbotts Ripton, NERC/ITE, 92–95. (ITE Symposium, 18). http://nora.nerc.ac.uk/policies.html#access

Halpern BS, Walbridge S, Selkoe KA et al (2008) A Global map of human impact on marine ecosystems. Science 319:948–952

Haroon AM (2022) Review on aquatic macrophytes in Lake Manzala, Egypt. Egypt J Aquat Res 48:1–12

Hogeweg P, Brenkert AL (1969) Structure of aquatic vegetation: a comparison of aquatic vegetation in India, the Netherlands and Czechoslovakia. Trop Ecol 10:139–162

Holm LG, Plocknett DL, Pancho JV, Herberger JP (1977) The world's worst weeds: distribution and biology. University Press of Hawaii, Honolulu, p 609

Kabata-Pendias A (2011) Trace elements in soils and plants, 4th edn. Taylor & Francis Group, Boca Raton, p 534

Khedr AA (1999) Floristic composition and phytogeography in a Mediterranean deltaic lake (Lake Burullus), Egypt. Ecologia Mediterranea 25:1–11

Kibar B, Temel S (2015) Evaluation of mineral composition of some wild edible plants growing in the eastern Anatolia Region grasslands of Turkey and consumed as vegetable. J Food Process Preserv 40:56–66

Klein H (2011) University of Alaska Anchorage: Alaska Center for Conservation Center (UAA, ACCC). Alaska Exotic Plants Information Clearinghouse (AKEPIC). Available: http://accs.uaa.alaska.edu/invasive-species/non-native-plant-species-list. Accessed 18 May 2016

Kłosowski S, Kłosowski G (2007) Aquatic and marsh plants. MULTICO Oficyna Wyd. [In Polish], Warsaw

Kumar V, Singh J, Kumar P (2020) Regression models for removal of heavy metals by water hyacinth (Eichhornia crassipes) from wastewater of pulp and paper processing industry. Environ Sustain 3:35–44. https://doi.org/10.1007/s42398-019-00093-x

Lee S, Kim K (2022) Effects of temperature on soil geochemical properties and accumulation of heavy metals in Brassica. https://doi.org/10.21203/rs.3.rs-1843160/v1

Leprieur C, Kerr YH, Mastorchio S, Meunier JC (2000) Monitoring vegetation cover across semi-arid regions: comparison of remote observations from various scales. Int J Remote Sens 21:281–300

Lorenzen B, Brix H, Mendelssohn IA, McKee KL, Miao SL (2001) Growth, biomass allocation and nutri-ent use efficiency in *Cladium jamaicense* and *Typha do mingensis* as affected by phosphorus and oxygen availability. Aquat Bot 70(2):117–133

Majid SN, Khwakaram AI, Mam Rasul GA, Ahmed ZH (2014) Bioaccumulation, enrichment and translocation factors of some heavy metals in Typha Angustifolia and Phragmites Australis Species growing along Qalyasan Stream in Sulaimani City /IKR. Journal of Zankoy Sulaimani- Part A . https://doi.org/10.17656/jzs.10350

Makarius CS, Lalika D, Mende H, Pia U, Doroth MG, Stewart JM, Gaudensia D (2013) Domestication potential and nutrient composition of wild orchids from two southern regions in Tanzania. Time J Biol Sci Technol 1:1–11

Massachusetts Department of Conservation and Recreation (MADCR). Office of Water Resources: Lakes and Ponds Program (2002) Available: http://www.mass.gov/eea/docs/dcr/watersupply/lakepond/factsheet/phragmites.pdf. Accessed Nov 2002

Mitsch WJ, Gosselink JG (2007) Wetlands, 4th edn. Wiley, New York, p 582

Mojiri A, Abdul Aziz H, Zahed MA, Aziz SQ, Selamat M (2013) Phytoremediation of heavy metals from urban waste leachate by Southern Cattail (Typha domingensis). Int J Sci Res Environ Sci (IJSRES) 1(4):63–70

Morari F, Dal Ferro N, Cocco E (2015) Municipal wastewater treatment with *Phragmites australis L* and *Typha latifolia L*. for irrigation reuse. Boron and heavy metals. Water Air Soil Pollut 226(3):56

Nabi M (2021) Heavy metals accumulation in aquatic macrophytes from an urban lake in Kashmir Himalaya, India. Environ Nanotechnol Monit Manag 16:100509

Nabi M, Dar SA (2022) Bioremediation: Microbial and plant assisted remediation of contaminated environments. In: Rani M, Chaudhary BS, Jamal S, Kumar P (eds) Towards sustainable natural resources, pp 175–193

Newman S, Grace JB, Koebel JW (1996) Effects of nutrient and hydroperiod on *Typha, Cladium* and *Eleocharis*: implications for everglades restoration. J Appl Ecol 6(3):774–783

Nin CJ, Rodgher S (2021) Effect of a temperature rise on metal toxicity for the aquatic biota: a systematic review. Brazilian Journal of Environmental Sciences 56(4):710–720. https://doi.org/10.5327/Z217694781010

Okbah MA (2005) Nitrogen and phosphorus species of Lake Burullus water (Egypt). Egypt J Aquat Res 31:186–198

Okbah MA, Hussein NR (2006) Impact of environmental conditions on the phytoplankton structure in Mediterranean Sea lagoon, Lake Burullus, Egypt. Water Air Soil Pollut 172:129–150

Ovalle AGC, Tristán AC, Amador-Nieto JA, Putri RF, Zahra RA (2021) Analysing the land use/land cover influence on land surface temperature in San Luis Potosí Basin, México using remote sensing techniques. The International Conference on Smart and Innovative Agriculture. IOP Conf Series: Earth Environ Sci 686:012029

Parastatidis D, Mitraka Z, Chrysoulakis N, Abrams M (2017) Online global land surface temperature estimation from Landsat. Remote Sens 9(12):1208. https://doi.org/10.3390/rs9121208

Peng K, Luo C, Lou L, Li X, Shen Z (2008) Bioac-cumulation of heavy metals by the aquatic plants *Pot-mogeton pectinatus* L. and *Potamogeton malaianus* Miq. and their potential use for contamination indicators and in wastewater treatment. Sci Total Environ 392(1):22–29

Peters JA, Lodge DM (2009) Litoral zone, encyclopedia of inland waters, reference module in earth system and environmental science. Academic, Cambridge, pp 79–87

Pignatti S (1982) Flora d'Italia. Edagricole, Bologna

Pillai P (2010) Accumulation of heavymetals from contaminated wastewater by aquatic plant Lemna minor and their biochemical effects on it. Nat Environ Pollut Technol 9(4):767–774

Pilon J, Santamaria L, Hootsmans M, van Vierssen W (2002) Latitudinal variation in life-cycle characteristics of Potamogeton pectinatus L.: vegetative growth and asexual reproduction. Plant Ecol 165:247–262

Rejmankova E (2011) The role of macrophytes in wetland ecosystems. J Ecol Field Biology 34(4):333–345

Roberts DA, Johnston EL, Poore AGB (2008) Contamination of marine biogenic habitats and effects upon associated epifauna. Mar Pollut Bull 56:1057–1065

Salem ZB, Laffray X, Ashoour A, Ayadi H, Aleya L (2014) Metal accumulation and distribution in the organs of reeds and cattails in a constructed treatment wetland (etueffont, France). Ecol Eng 64:1–17

Serag MS (1996) Ecology and biomass of *Phragmites australis* (Cav.) Trin. Ex Steud. In the north-eastern region of the Nile Delta, Egypt. Ecoscience 3(4):473–482

Serrano J, Shahidian S, da Silva JM (2019) Evaluation of normalized difference water index as a tool for monitoring pasture seasonal and inter-annual variability in a Mediterranean Agro-Silvo-pastoral system. Water 11:62. https://doi.org/10.3390/w11010062

Shaltout KH, Al-Sodany YM (2008) Vegetation analysis of Burullus Wetland: a AMSAR site in Egypt. Wetlands Ecol Manage 16(5):421–439

Shaltout KH, Khalil MT (2005) Lake Burullus (Burullus protected area). Publication of National Biodiversity Unit (NBU) No 13. Egyptian Environment Affairs Agency (EEAA), Cairo, 578 p

Smith SG (1962) Natural hybridization among five species of cattail. Am J Bot 49:678

Smith SG (1967) Experimental and natural hybrids in North America Typha (Typhaceae). Am Midl Naturalist J 78:257–287

Solanky V, Singh S, Katiyar SK (2018) Land surface temperature estimation using remote sensing data. In: Singh V, Yadav S, Yadava R (eds) Hydrologic modeling. Water Science and Technology Library, vol 81. Springer, Singapore. https://doi.org/10.1007/978-981-10-5801-1_24

Täckholm V (1974) Student's flora of Egypt, 2nd edn. Cairo Univ. Press, Cairo, pp 888

UKMO: UK Met Office (2013) Climate: observations, projections and impacts: Egypt. USAID, Climate Change Information Fact Sheet EGYPT

UNESCO (1977) Map of the world distribution of arid regions. MAB Technical Notes 7

van Wijk RJ (1988) Ecological studies on Potamogeton pectinatus L. I. General characteristics, biomass production and life cycles under field conditions. Aquat Bot 31:211–258

Vodyanitskii YN, Shoba SA (2015) Biogeochemistry of carbon, iron, and heavy metals in wetlands (analytical review). Mosc Univ Soil Sci Bull 70(3):89–97

Wolverton BC, McDonald RC (1978) Bioaccumulation and detection of trace levels of cadmium in aquatic systems by *Eichhornia crassipe*. Environ Health Perspect 27(1):161–164

Xing W, Wu H, Hao B, Huang W, Liu G (2013) Bioaccumulation of heavy metals by submerged macrophytes: looking for hyperaccumulators in eutrophic lakes. Environ Sci Technol 47:4695–4703. https://doi.org/10.1021/es303923w

Xu H (2006) Modification of normalized difference water index (NDWI) to enhance open water features in remotely sensed imagery. Int J Remote Sens 27(14):3025–3033

Yu L, Longqing L, Qiang Z, Yiming Y, Heling W, Ruijun W, Jihui Z (2013) Influence of temperature on the heavy metals accumulation of five vegetable species in semiarid area of northwest China. Chem Ecol 29(4):353–365. https://doi.org/10.1080/02757540.2013.769970

Zahran MA, Willis AJ (2009) The vegetation of Egypt, 1st edn. Chapman and Hall, London, pp 424

Zhang F, Zhou G (2019) Estimation of vegetation water content using hyperspectral vegetation indices: a comparison of crop water indicators in response to water stress treatments for summer maize. BMC Ecol 19:18. https://doi.org/10.1186/s12898-019-0233-0

Zhang R, Sutton R, Danabasoglu G, Kwon Y, Marsh R, Yeager SG, Amrhein DE, Little CM (2019) A review of the role of the atlantic meridional overturning circulation in atlantic multidecadal variability and associated climate impacts. Rev Geophys 57(2):316–375

Zhou C, Chen S, Zhang Y, Zhao J, Song D, Liu D (2018) Evaluating metal effects on the reflectance spectra of plant leaves during different seasons in post-mining areas, China. Remote Sens 10:1211. https://doi.org/10.3390/rs10081211